5 Exploratory Analysis of Event-Related fMRI Demonstrated in a Working Memory Study

Andrzej Wichert, Henrik Walter, Jo Grothe, and Birgit Abler
Department of Psychiatry
University of Ulm, D-89075 Ulm, Germany
wichert@neuro.informatik.uni-ulm.de
{henrik.walter, jo.grothe, birgit.abler}@medizin.uni-ulm.de

Friedrich T. Sommer
Department of Neural Information Processing
University of Ulm, D-89069 Ulm, Germany
fritz@neuro.informatik.uni-ulm.de

Here we describe a novel technique for exploratory analysis of event-related fMRI. The technique comprises two parts. The first component is dense latency sampling (DLS), an oversampling scheme for event-related fMRI that has the advantage of providing volume slice timing without the need for signal interpolation. The second component is dynamical cluster analysis (DCA) of signal time-courses; this analysis is done with temporal constraints taken from the event-related design: Signal segments that correspond to different types of events are analyzed separately to reveal specific event-related activation. The technique does not rely on preassumptions about the temporal shape of functional activity like common inerential methods.

We demonstrate the utility of the technique and also compare its performance to standard techniques in a study of working memory. The technique reveals spatio-temporal patterns of activity associated with different memory load conditions. Most delay-related activity appeared in parietal and prefrontal regions peaked in the second half of the delay period; this suggested involvement of these regions in processes of memory rehearsal and decision making. The superior parietal and precentral cortices also participated in delay-related activity. But for these regions the temporal shapes of functional activation suggested additional roles in memory encoding.

5.1 Introduction

Almost all methods of data analysis in fMRI make assumptions about the nature of the underlying neuronal processes. The methods can be divided into two classes, based on the type of assumptions made. One class of methods uses univariate analysis and relies on the assumption of functional specialization of cortical regions. The other class employs multivariate analysis and relies on the assumption of functional integration, that is, that brain function results from cooperative interactions among cortical regions. Here, we will describe a technique, belonging to this second class, that applies multivariate analysis to data from event-related fMRI (ER fMRI). Our approach of exploratory data analysis is designed to detect weak, task-induced signal changes whose shapes are not known beforehand (Wichert et al., 2001a,b). The technique combines a new scheduling scheme of multi-slice data acquisition with a variant of temporal cluster analysis. The approach is designed for complex experimental paradigms with short events where the event-related signal is weak and has a time course that is difficult to predict. Studies that explore cognitive processes like memory typically involve such complex paradigms.

In order to evaluate the strength of our technique we chose the study of working memory. The choice of this cognitive task made sense for two different reasons. First, working memory is amenable to study with our technique because the timing of the neural processes it involves can be directly manipulated by experimental design. Second, earlier studies had indicated that the formation of working memory is distributed across disparate cortical areas, thus, suggesting that functional integration might be important.

The concept of working (or short term) memory refers to a type of memory that has limited capacity for storing and manipulating information necessary for performing a specified task. It was originally defined in studies in which subjects were presented with a list of items and then asked to recall individual entries on the list. Results from these studies defined the upper limits of memory load, i.e., the maximum number of items (such as words) that could be memorized with reasonable accuracy. Typically, experiments test working memorizes whose durations range from a few seconds to a few minutes. The mechanisms of working memory vary as a function of the length of time the memory is required to last. If the duration is short, 10s or less, subjects recall items nearer the end of the list more accurately that those at the beginning of the list. This recency effect disappears if the duration of the memory exceeds 10s. Thus, there seems to be a qualitative difference between memories that persist for more 10s and those that are briefer — the former are more durable than the latter.

A common type of task used in studies of working memory is called delayed match-to-sample task or simply delayed response task. The task consists of three discrete phases. The first is a presentation phase during which the subject is presented with a set of items to memorize (the memory set). The presentation phase is followed by the delay period, an interval during which no tasks are required. The

last phase is the probe phase during which the subject is presented with an item and must decide whether or not it belongs to the memory set.

The cellular neurophysiology of delayed response tasks has been studied in experiments with animal models. These studies showed that prefrontal and parietal cortical region are involved in working memory. Cells in these regions respond selectively during different phases of the task, indicating "process specificity" (Baddeley, 1986, 1996). For instance, a population of cells in prefrontal cortex fire persistently during the delay phase. Cells in prefrontal cortex are also able to convey information about both the identity and location of a given item in a memory set (Rainer et al., 1998).

Whole-brain neuroimaging techniques such as PET and fMRI promise to reveal the global functional architecture of working memory (Jonides et al., 1993; D'Esposito et al., 1995; Goldman-Rakic, 1996; Owen et al., 1996; Postle et al., 2000b; Goldman-Rakic, 2000). The first neuroimaging studies of working memory made only indirect assessments of functional activity (Cabeza and Nyberg, 2000). The advent of the event-related fMRI technique (Josephs et al., 1997; Dale and Buckner, 1997) gave direct access to the functional activity caused by short events such as a single delayed response task. These later studies led to revisions of theories of working memory that had been based on results from the indirect assessments (Postle et al., 2000a). Thus, the evolution of methods in whole-brain imaging allows the refinement and revisions of theories of brain function.

In the study of working memory that we will describe we will focus on the following three questions. i) How do results depend on the paradigm used in data analysis, specifically, do results change if one switches from the assumption of functional specialization (underlying common univariate inferential fMRI data analysis) to the assumption of functional integration (the incentive of multivariate exploratory fMRI data analysis)? ii) How do the time courses of functional activity relate to results from single-cell recordings? iii) Are sensory areas involved in the delay phase?

All told, the overall aims of the chapter are to explain our data acquisition and analysis technique, to discuss its relations to other approaches in ER fMRI, and to evaluate its ability to explore processes of working memory. The results of the new technique will be compared with those of state-of-the-art approaches, i.e., the slice timing technique usually applied in multi-slice fMRI, and conventional inferential data analysis by the general linear model (GLM). The discussion of the results of our study in the context of earlier working memory literature will be brief and certainly not cover all aspects. A more exhaustive description of the results will appear in a forthcoming paper.

5.2 Current Methods for Event-Related fMRI

5.2.1 New Chances and Challenges

The classical block design common in PET and early fMRI introduced stationary phases of functional activation (blocks). The stationarity requirement posed strong limits on the investigation of behavioral paradigms. A considerable widening of the scope of neuroimaging was provided by the introduction of ER fMRI registration technique. In ER fMRI the data aquisition is exactly scheduled relative to events in the experimental design. Thus, it allows to register signal changes evoked by short events, quite similar to evoked event-related potentials measured with EEG/MEG. Of course, with regional blood flow imaging techniques the temporal resolution is generically limited by the delayed and low-pass filtered hemodynamic response (HR) (with time-to-peak interval of about 5s). However, up to the generical resolution limit, ER fMRI provides more freedom for implementing experimental paradigms. For instance, short events can be repeated in random order, or categorized post-hoc. Early studies using the event-related technique were on odd-ball paradigms (MCarthy et al., 1997) and on various cognitive paradigms (for short comprehensive reviews, see (Buckner, 1998; Rosen et al., 1998)). In the performance of cognitive tasks, ER fMRI allows to discern and characterize different phases that were only indirectly assessible in block designs.

The extended scope of ER fMRI implicates as well new difficulties in data analysis. For inferential analysis the availability of an adaequate regressor or model function for functional activation, determined external to the data, is an indispensable prerequisite (Lange, 1996, 1997; Lange et al., 1999; Petersson et al., 1999a,b). The regressors used for block designs are box-car functions reflecting the blocks, convolved by a canonical HR (Bandettini et al., 1993). If the durations of blocks are long compared to the HR characteristic, exact modeling of the HR is uncritical for the inferential analysis. For event-related designs the situation is entirely different. The time course of functional activity is not as completely prescribed by the experimental paradigm as in block design. Thus adaequate regressor functions necessary to detect the weak component of functional activity[1] are hard to predict independently of the fMRI data. A method to estimate adaequate regressor functions from the fMRI data set is revisited in the following paragraph.

1. The typical S/N of functional imaging in an 1.5T scanner is 1-5%. Regression analysis with the box-car shaped regressor function reflecting the block design reduces the noise by temporal averaging within blocks.

5.2.2 Signal Averaging and Data Analysis

To achieve a noise reduction in ER fMRI *selective averaging* has been proposed by Dale and Buckner (1997):

$$h = X^T y \tag{5.1}$$

where h is the sampled HR, y stands for the signal measured at a voxel, and X is the design matrix reflecting the event timing during the experiment.

Current inferential data analyses for ER fMRI uses families of regressor functions generated by a canonical HR impulse response function systematically shifted in time. Since for short events the sensitivity of the analysis depends critically on a good model of the HR, Dale (1999) had proposed to estimate the HR response from the data set to be analyzed. He used univariate linear signal estimation based on ordinary least square (OLS) fits

$$h_{OLS} = (X^T X)^{-1} X^T y, \tag{5.2}$$

To take into account influences between events, Burock and Dale (2000) employed univariate linear signal estimation based on maximum likelihood (ML) estimation:

$$h_{ML} = (X^T C_n^{-1} X)^{-1} C_n^{-1} X^T y. \tag{5.3}$$

where C_n denotes the covariance of the noise. Burock and Dale (2000) used equation 5.3 as regressor in a modified approach of inferential data analysis.

5.2.3 Increased Resolution by Oversampling

In state-of-the-art fMRI scanning the lower limit on the repetition time (TR) is methodologically prescribed. Since different slices cannot be acquired simultaneously, TR grows proportionally with the number of slices in the measurement volume. Because the time constant of spin relaxation is fixed, the time required for a slice measurement cannot be arbitrarily reduced. The current limit is about $TR \simeq k \times 80$ ms, with k the number of slices. As first suggested for cardiac fMRI, oversampling can virtually increase the intrinsically low temporal resolution of multi-slice ER fMRI[2]. Oversampling means that each type of event is recorded repeatedly, say r times, each event repetition sampled with a different latency. The sampling time points can either be randomly jittered, or equidistantly distributed in the interval TR. The latter we refer to as *equidistant oversampling*. In such sampling schemes the latency is varied between 0 and $TR(1 - 1/r)$ in steps of TR/r which increases the effective sampling rate from $1/TR$ to r/TR. Josephs et al. (1997) first proposed equidistant oversampling for neuro fMRI (with $r = 2$). The method was used for estimating HR functions (Miezin et al., 2000).

2. Oversampling critically relies upon the condition that repeated trials produce similar functional activation, an assumption also made in conventional fMRI.

5.2.4 Slice-Timing

The technical limitation in multi-slice fMRI that different slices cannot be recorded simultaneously causes the *slice timing problem*. This describes the fact that a recorded volume is not an instantaneous picture in time. The different slices are recorded one after another in intervals of TR/k. While negligible with traditional block designs, the slice timing differences matter for the investigation of event-related designs.

The current method to solve this problem is a procedure called volume slice timing that involves phase-shift manipulations in the data: A reference slice is selected in the volume and all signals measured in other slices are phase-shifted[3] to the sampling points of the reference slice, see figure 5.1 a). Because the required shifts of the phases are smaller than the sampling intervals of the signals, this manipulation involves signal interpolation and the typical errors associated with it, such as ringing and wrap-around effects, see (Schanze, 1995). The described procedure is applied as a standard preprocessing step, often even before inferential data analysis, where in principle the slice timing could be reflected more properly by shifting the regressors for each slice individually (Josephs et al., 1997).

5.3 Exploratory Analysis in Functional Imaging

For multivariate exploratory analysis of fMRI/PET data various methods have been proposed, such as principal component analysis (Lai and Fang, 1999; Hansen et al., 1999; Baumgartner et al., 2000a), indepedent component analysis (McKeown et al., 1998; McKeown and Sejnowski, 1998; McKeown et al., 1999), and diverse temporal clustering methods (Scarth et al., 1995; Baumgartner et al., 1997; Golay et al., 1998; Baune et al., 1999; Goutte et al., 1999; Filzmoser et al., 1999; Fadili et al., 2000), and see chapter Somorjai and Jamusz. The goal of these approaches is to detect characteristic spatio-temporal properties in the data as much as possible uninformed of a priori assumptions about the results.

Exploratory data can yield a reduced data set that still reflects the important properties in the data. For instance, cluster analysis approaches in functional imaging usually apply *temporal cluster analysis* (TCA) i.e., they cluster the data with respect to the shapes of the signal time courses. TCA partitions the data into sets of voxels with similar time courses—clusters[4]. A cluster can be characterized by its *spatial pattern* and by the *cluster center*, that is, the averaged time course.

3. Applying the Fourier-shift theorem, a phase shifting can be achieved by multiplying with a complex exponential in Fourier space (Aguirre et al., 1998).
4. It has to be emphasized that a cluster resulting from temporal TCA is different from a spatially contiguent set of voxels (for instance, in functional maps), often referred to as cluster. The first collates voxels of similar signal shape, but completely independent of spatial positions. To avoid confusion we will refer to the latter as a spatial cluster.

Exploratory data analysis was successfully applied for block design experiments, see the comparison between different exploratory and inferential data analysis approaches in (Lange et al., 1999). However, few attempts have been made to apply exploratory data analysis to ER fMRI, but see (Richter et al., 2000). For ER fMRI, where inferential data anlysis is hampered by the lack of adaequate regressors, exploratory data is particularly interesting.

5.4 New Technique for Exploratory Analysis of Event-Related fMRI

In this section we describe a new approach to characterize functional activity in event-related fMRI. It relies on selective signal averaging as well, but applies exploratory analysis techniques (section 5.3) rather than univariate signal estimation and inferential data analysis described in section 5.2.2. The first part of this section, section 5.4.1, explains the data acquisition method, the second part, section 5.4.2, the exploratory analysis algorithm and its application to ER fMRI data.

5.4.1 Data Acquisition and Slice Timing

5.4.1.1 Dense Latency Sampling

For increased temporal resolution we use equidistant oversampling of events as described in section 5.2.3. Applying selective averaging (equation 5.1) after equidistant oversampling yields signal time courses virtually sampled with a rate of r/TR.

Equidistant oversampling can have another interesting consequence for multi-slice data acquisition that, as far as the authors are aware, has not been exploited before: With the sampling rate chosen appropriately it can also resolve the slice timing problem described in section 5.2.4; for $r = k$, that is the number of repeated events is equal to the number of acquired slices, a dense sampling can be guaranteed. Dense sampling means that for any slice measurement all the $k-1$ other slices completing a volume have been recorded with the same latency during other repetitions of the event. Thus, slice timing can be achieved just by data re-sorting, i.e., by rearranging slices of same acquisition latency to new volumes. Re-sorting is done with respect to a labeling of the measured data based on the event-related design matrix. Each slice is labeled by the latency between the exact acquisition time and the event with the largest influence on the signal. The labeling takes into account an assumed delay until the maximum effect of an event is expressed in the HR. We used a 5s time-to-peak interval of the canonical HR. The described methods are explained by schematic pictures in figure 5.1.

The combination of equidistant dense sampling scheme and data re-sorting we call the *dense latency sampling (DLS)* technique (Wichert et al., 2001b). Like in conventional ER fMRI the DLS technique leaves the freedom to schedule order and onsets of events in the experiment in a pseudorandom manner. The advantage of the DLS fMRI technique is that it provides volume slice timing without introducing

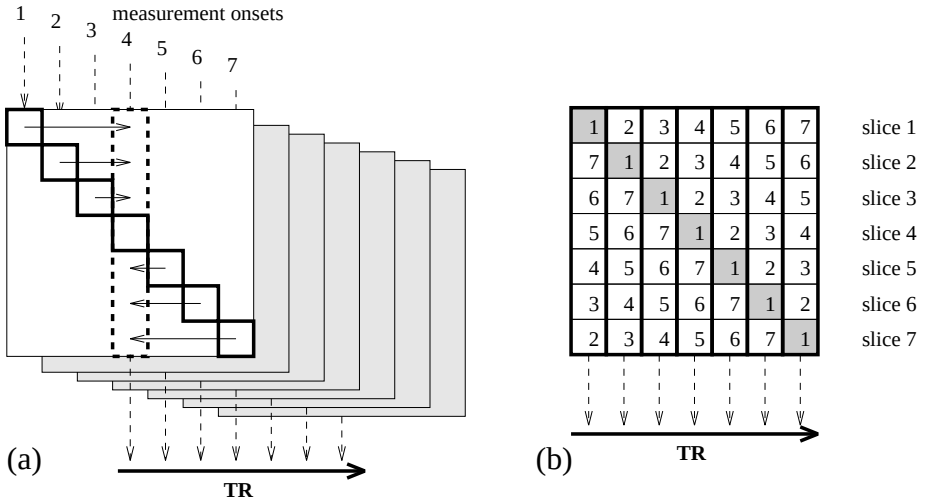

Figure 5.1 Schematic views of the DLS method and phase-shift slice timing (example with $k = 7$ slices per volume and $r = 7$ event repetitions). Picture a) shows the DLS data acquisition scheme and the effect of phase-shift slice timing: Big squares symbolize the acquisition of volumes. The horizontal extension corresponds to the acquisition time TR, the vertical extension to the spatial axis perpendicular to the measured slices (as labeled on the right margin of the figure). The shaded squares in the background sketch volume measurements taken at event repetitions. Latencies between events and measurements were varied such that the interval of TR (marked by the bold horizontal arrow) is equidistantly divided by sampling points (depicted by the downward arrows). Thus, the oversampling rate is TR/r. Within the acquisition volume in the foreground the small squares symbolize how different slices are measured one after the other. The thin horizontal arrows depict the effect of phase-shift slice timing (with slice 4 chosen as the reference slice), the dashed rectangle symbolizes the resulting slice-timed volume. Picture b) shows the result of the DLS-re-sorting. Bold rectangles denote the volumes assembled by re-sorting with respect to the latencies between event and the individual measurements. The numbers indicate the event repetition from picture a) indicating the origin of each slice. In addition, the slices acquired during the first event are marked by shaded squares—they are distributed over different DLS volumes. Note, that the choice $r = k$, provides complete volumes at each sampling point after re-sorting.

artifacts of the conventional slice-timing procedure (section 5.2.4). Particularly for designs with long repetition times TR, when phase-shift artifacts become more and more serious, the DLS technique offers an interesting alternative for slice timing. A reliable method for volume slice timing is crucial for all sorts of exploratory analysis methods such as principal/independent component analysis and cluster analysis.

5.4.1.2 Dense Latency Sampling at Lower Rates

As explained before, the full DLS technique requires an oversampling rate TR/r equal to the single-slice sampling rate of the used measurement sequence. For complex experimental paradigms, however, this requirement results in long durations

of experimental sessions. In such cases one might prefer a lower effective temporal resolution, if achieved with fewer event repetitions.

A reduction of the sampling rate required for data re-sorting is possible by combining DLS-fMRI with modest phase-shifting. The idea is to apply phase-shift time slicing not only with respect to a single reference slice per volume. Instead one can choose $s > 1$ reference slices spaced equidistantly over the volume. For each slice only the data corresponding to the closest reference slice are used. These can be arranged to complete volumes by DLS re-sorting as explained in section 5.4.1.1. Compared with the traditional phase-shift slice timing the resulting interpolation errors are smaller because the maximum phase-shifts involved are reduced from $TR/2$ to $TR/(2s)$[5]. The combination of DLS-technique and phase-shifting can be best explained with an example: For a measurement volume consisting of $k = 21$ slices, phase shifting is done for the reference slices $2, 5, 8, 11, 14, 17$, and 20. The result is $s = 7$ slice-timed zones in the volume, each zone comprising three adjacent slices. The situation is again reflected by figure 5.1 where now each slice corresponds to a zone of 3 slices and the measurement latencies stand for the latencies of the reference slices. By DLS-re-sorting one can rearrange the different zones to complete slice-timed volumes. In this example the maximum phase-shift to be applied to the data is reduced from $10 \times TR/21$ in the standard slice timing technique (using slice 10 as reference slice) to $1 \times TR/21$ with the DLS technique. Thus, the required event repetitions, as well as the effective sampling rate were reduced by a factor of 3 compared with the full DLS-scheme.

5.4.2 Exploratory Analysis for Event-Related fMRI

5.4.2.1 Restricted Cluster Analysis

The results of multivariate exploratory analyses like temporal cluster analysis (TCA) depend on the selection of voxels included in the analysis. Therefore, removal of voxels outside the brain using a simple threshold criterion for the mean signal amplitude is a usual preprocessing step. The most assumption-free way to perform data exploration is then to run TCA on the whole brain volume and over the entire sequence of slice-timed volumes. While this provides a screening of the data for detecting coarse artifacts, not all functionally induced spatio-temporal structure might be segregated in clusters under such a broad scope. Particularly, event-related responses, short in duration, and interspersed with regard to event type, are unlikely to be detected by unrestricted TCA.

TCA can be restricted in space and time. By applying TCA only in a partial volume of the brain one can focus on regions of interest, or disregard regions of

5. To further minimize interpolation errors, recent techniques such as the expansion with phase-invariant Fourier-sets as base functions, or the inclusion of temporal derivatives could be used, see (Henson et al., 1999; Josephs and Henson, 1999).

no interest. For uncovering functionally related structure more specifically, one can restrict TCA in the time dimension, i.e., inspect temporal segments of the data that have been selected informed by the experimental paradigm. We used temporal restriction for isolating effects from experimental conditions, in our case, from different event types. The selection of segments to be analyzed used the labeling of the measurement sequence as described in section 5.4.1.1 (Wichert et al., 2001a).

In the reminder of this section we will briefly describe two more technical topics that are essential components of the data analysis technique, the clustering method (section 5.4.2.2), and definitions of temporal and spatial similarity we used in the cluster analysis and to assess and compare the clustering results (paragraph 5.4.2.3). After TCA is carried out for each conditions independently, these similarity measures can be used to search for relations and differences in functional activity of different conditions.

5.4.2.2 Dynamical Clustering

As a number of previous studies have revealed, the standard clustering algorithm, k-means clustering is not the right choice for high-dimensional fMRI data sets (with hundreds of sampling points in time). The gradient-descent performed by the k-means algorithm is a local minimizer that for high-dimensional data sets frequently fails to find the global minimum, resulting in poor data fits. An indicator for the local minima problem of k-means clustering is a poor reproducability of the results. The results depend strongly on the initialization of the cluster centers. With random initialization[6] repeated runs of k-means clustering on the same data set can lead to quite different partition results.

Therefore, alternative algorithms have been proposed, like fuzzy clustering (Scarth et al., 1995; Moser et al., 1997; Baumgartner et al., 1997; Golay et al., 1998; Fadili et al., 2000), hierarchical clustering (Goutte et al., 1999; Filzmoser et al., 1999), and dynamical cluster analysis (DCA) (Baune et al., 1997, 1999). In DCA the number of clusters is not fixed like with k-means clustering; cluster centers are generated and anihilated during the data fitting process. A comparison between k-means CA and DCA has shown that the reproducability of DCA is much better (Baune et al., 1999). The problem with DCA is that it is computationally expensive. The advantage of dynamical cluster generation in DCA led us to a variant of k-means clustering with dynamical initialization phase for the choice of cluster seeds, very similar as the one proposed by Waldemark (1997). For a previously specified radius r the initialization phase generates a set of cluster seeds such that for every data point at least one of the seeds is closer than r. The initialization is completed after a single sweep through the data set where successively each data point is assigned as cluster seed if all previously assigned seeds are farther away

6. In random initialization, the default used for k-means clustering, k data points are picked at random as seeds for the cluster centers.

than r. We will refer to the combination of k-means clustering with the described dynamical initialization phase as K-MDI clustering. On the data of the working memory study both methods, K-MDI and DCA, achieved similar results, but the first was considerably faster. Therefore, in the following we will only report the results provided by K-MDI clustering.

5.4.2.3 Assessment and Comparison of Cluster Solutions

TCA requires one strong a priori assumption which is the measure of *temporal dissimilarity (td)* used for clustering. We used the Euclidean distance between two time courses. Another commonly used measure, that only compares signal shapes and entirely disregards absolute signal amplitudes, is based on the correlation coefficient.

After completion of TCA there is the problem how to inspect, assess and interpret the results in a systematic and fair manner. This requires quantitative description of the results, i.e., of the properties of centers and spatial patterns of the clusters. The *td* measure used during clustering can also be applied post hoc to the cluster centers for assessing differences in the temporal signal shape. In addition, we used the following definitions (Wichert et al., 2001a): The *signal change homogeneity (SCH)* which is defined as the ratio between peak-to-peak amplitude of the cluster center and mean standard deviation of signal amplitudes of the members of a cluster. The *temporal smoothness (TSM)* which is defined as the relative spectral power in the low frequency range of a time course. The *spatial contiguity (SC)* which is defined as the relative number of adjacent voxels in a voxel set (presence of "spatial clusters"). The *spatial similarity* ($0 \leq ss \leq 1$) between two patterns which is defined as the normalized overlap, i.e., the ratio between the numbers of voxels in the intersection and the union of the voxel sets corresponding to the clusters. For a pattern b and a pattern set A we call $a \in A$ *best match to* b, if a is the element with maximum spatial similarity to b. For two pattern sets A and B we call $a \in A, b \in B$ *best-matching pair*, if a is best match to B and b is best match to A.

For inspection and interpretation of clustering solutions we select clusters based on threshold criteria using the introduced measures. Functional activation can be assessed by focussing on clusters with high values in SCH and TSM. The first criterion selects clusters whose voxels homogeniously display signal changes of the cluster center. To assess homogeneity of time courses in fMRI activity maps Kendall's coefficient of concordance has been proposed (Baumgartner et al., 1999, 2000b). We prefer the SCH measure for cluster selection because it measures the homogeneity of signal changes which are essential for characterizing functional activity [7]. A threshold on TSM is used to reject clusters whose signal shape cannot be explained by influences mediated by the low-frequent HR.

7. For visual inspection of cluster homogeneity we display cluster centers with error bars reflecting standard deviation of signal amplitudes of the members.

As an optional selection criterion one can require high SC. This rules out clusters whose spatial patterns are scattered. Such rejection follows a common assumption that meaningful fMRI activity occupies a larger region than the volume of a single voxel (typically $1 \times 1 \times 3$ mm^3) and thus forms a *spatial cluster*[8]. This assumption also underlies spatial smoothing of the data, a preprocessing step, that is often applied before starting with data analysis (Xiong et al., 1995). Spatial filtering, for instance, with Gaussian kernels, enhances contiguous components in the signal by spatial averaging. In our technique spatial clustering is used as post hoc criterion to assess the result of temporal clustering[9].

The measures ss and td will be used for various comparisons between conditions. For instance, cluster results from two different conditions can be checked for spatial similarity. A spatially corresponding cluster pair (a best-matching pair) suggests that similar regions are recruited by both conditions. Differences in the centers of corresponding clusters indicate condition-specific changes of functional activation. Size differences of corresponding clusters, however, cannot be interpreted directly. Due to the global nature of the clustering process, the size of a cluster is influenced by push-away effects from other clusters[10].

5.5 The Working Memory Study

5.5.1 The Experimental Task and Data Aquisition

Five male and four female volunteers performed a delayed match-to-sample task in the fMRI scanner. Experiment blocks consisted of 42 task events with two different event types pseudo-randomly shuffled, one with low memory load (memory set with 1 letter) and one with high load (6 letters). Each event type occurred $r = 21$ times during one experimental block. An event started with the visual presentation of the memory set, a 2×3 array of the letters. For low load, a single letter to be memorized in the array was marked with a different color. The presentation lasted for 1s and 3.5s for low and high load, respectively. To reduce confounding effects in the following delay phase we adjusted memory set presentation time according to the number of items to be remembered (0.5s per item plus 0.5s) as usually done in behavioral studies (Richardson et al., 1996; Neath et al., 1999). After the delay

8. It is important to distinguish between spatial clusters, defined by voxel contiguities in spatial patterns, and the clusters extracted by clustering signal time courses as described in section 5.4.2.2. The latter are formed without any information about voxel contiguity. If the voxel pattern forms a spatial cluster this reflects the additional property that similar time courses are found in nearby voxels.

9. We apply spatial smoothing for preprocessing only before group averaging to account for imprecision of realignment and normalization and for interindividual differences in functional localization.

10. Neighboring clusters will compete for data points, resulting in a repulsive interaction.

period of 6s, a second visual stimulus was presented for 1.5s. It displayed a similiar 2×3 array containing one letter and five dummies. The subject had to press a yes/no button deciding whether or not the letter was in the memory set previously seen. Video goggles were used for visual presentation.

An experimental session consisted of two identical pseudorandom event blocks, as described above. For one male subject the experiment block was repeated five times. This data set was used in the single subject analysis. Data aquisition was performed on a 1.5 T Siemens Vision scanner. A full brain volume consisted of $k = 21$ slices and was sampled with TR = 1.9s.

5.5.2 Data Preprocessing and Analyses

We started data processing by motion correction using the realignment procedure in SPM99 (http://www.fil.ion.ucl.ac.uk/spm). In a second step for each subject the signals from repeated blocks were averaged. For assessing group effects the data of eight subjects (four male and four female) where spatially smoothed (with a Gaussian kernel of 8mm), normalized to the SPM Epi template, and averaged. Having performed the experiment with the DLS-fMRI technique described in section 5.4.1.1, there were two options for volume slice timing, DLS-re-sorting, or the usual phase-shift method. DLS-re-sorting was provided by a self-implemented program. For the purpose of comparison we also carried out the second option: The common signal interpolation slice timing was performed by the routine available in SPM99. Both, the phase-shifted and the DLS-re-sorted data set were analyzed in two different ways. We will use the following descriptors for different exprimental conditions: H denotes the high and L the low load condition in the working memory task. Different phases in the trials are denoted by s for memory set presentation, d for delay phase, and t for the test or probe phase. Thus, the set of different experimental conditions is $\mathcal{C} = \{Hs, Hd, Ht, Ls, Ld, Lt, P\}$, with P denoting pauses between events.

For inferential data analysis regression analysis in the GLM was carried out with SPM99. As regressors we used the box cars of the distinct experimental periods, stimulation, delay and target, convolved with a canonical HR function, a gamma function with a time-to-peak constant of 5s. The contrast functions we used in the GLM will be given in the result sections using a notation with the elements of $\mathcal{C}$. For instance, $Hd - Hs$ denotes the contrast function requiring a higher signal in the delay than in stimulus during the high load condition.

Cluster analysis was applied on different temporal segments of the data sets. For overall data exploration we applied TCA on $H\&L$, the data set containing the measurements during both load conditions. Such overall data exploration revealed for eight of the nine subjects scanner artifacts localized in the basal parts of the brain. For assessing group effects we disregarded the regions with distorted signal in the further analysis by spatial restriction of the cluster analysis. As described in section 5.4.2.1, we applied TCA separately on two data segments: L with a duration of 12s corresponding to the low load event; and H with a duration of 13.5s

corresponding to the high load event. The cluster analyses yielded 20 clusters for low load, and and 18 clusters for high load. In the following, these cluster sets will be labeled by $L1 - L20$, and $H1 - H18$, respectively.

5.5.3 Results for a Single Subject

This section compares the results from different data acquisition and analysis techniques for a single subject. The two most contrasting analysis approaches we employed were linear regression analysis (GLM) on the phase-shifted data set, as the most conventional, and K-MDI clustering on the DLS-data, as the most unconventional. If these extremes yielded agreeing results, we will not describe the results produced by intermediate approaches, such as TCA on phase-shifted data, or linear regression in the DLS data set. Overall data examination with TCA revealed no obvious artifacts so that the whole data set could be examined.

Our first question concerned visual functional activity. In the GLM we looked for voxels showing the same activation pattern in both load conditions, a higher signal intensity under visual stimulation, in the periods s and t, than without visual stimulation in the delay periods d. The binarized SPM_t map is shown in figure 5.2.

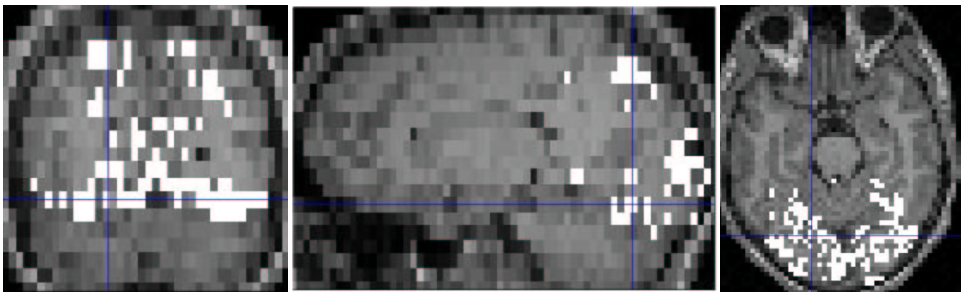

Figure 5.2 The SPM_t map of the contrast function $+Ls - Ld + Lt + Hs - Hd + Ht$ (corrected with $p < 0.05$) in the signal interpolation slice-timed data.

TCA was applied on the $H\&L$ DLS-data. For comparison with the results of standard GLM analysis we selected those clusters from the clustering result whose centers had highest temporal similarity with the used contrast function[11]. Note, however, that the selection of visual clusters was done post hoc, i.e., the formation of clusters was uninformed of any target function. The spatial maps of the two visual clusters are displayed in figure 5.3. The two clusters had very similar signal shape but different signal amplitude levels.

11. A boxcar function convolved with a canonical HR function.

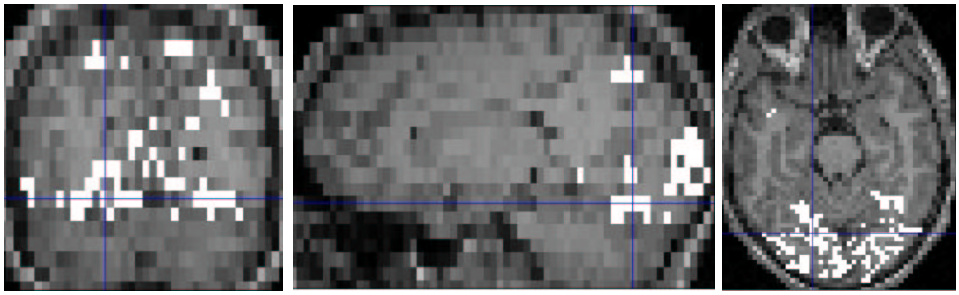

Figure 5.3 The clusters with highest temporal similarity to the contrast used in the SPM_t map displayed in figure 5.2.

Figures 5.2 and 5.3 show quite similar spatial maps for visual stimulation indicating that the time courses of visual stimulation were well preserved by both time-slicing operations. Further, this result suggested that visual activity is so dominant in the data statistics that it is lumped together even by a data exploration completely uninformed about the functional paradigm.

Our second question addressed delay activity, the focus of our study. We concentrated on the high load, using the contrast function $-Hs + Hd$, and masked the SPM_t map exclusively by two other contrast maps: stimulus deactivation against the baseline, i.e., $-Hs + P$, and second, higher delay activity during low load than during high load, i.e., $+Ld - Hd$. For the single subject this search was negative, neither in the slice-timed, nor in the DLS data set we were able to find significant delay activity with SPM or the exploratory analysis technique. Our negative result of finding delay-related functional activity in the single subject is in line with some previous fMRI studies of working memory fMRI, however, there are also studies reporting positive results.

Finally, we asked about functional activity related to both phases, delay period s and probe phase t. We applied a contrast including target and delay in both conditions against baseline $+D + T - P$. The obtained SPM_t map was exclusively masked by the contrast function for visual activation (cf. Figs. 5.3 and 5.4). The resulting map on the phase-shift slice-timed data is displayed in figure 5.4. Functional activity is scattered but shows higher spatial density in left parietal regions and bilateral prefrontal regions.

To assess the influence of the slice timing methods on such a smaller effect, we analyzed the DLS-re-sorted data set with the equivalent contrast function, see figure 5.5. Although the main spatial clusters agree, the maps differ in detail. There is less lateralization in the DLS-re-sorted data set than in the phase-shift slice-timed data set. This example shows that effects less salient than visual stimulation are influenced by the method of time-slicing.

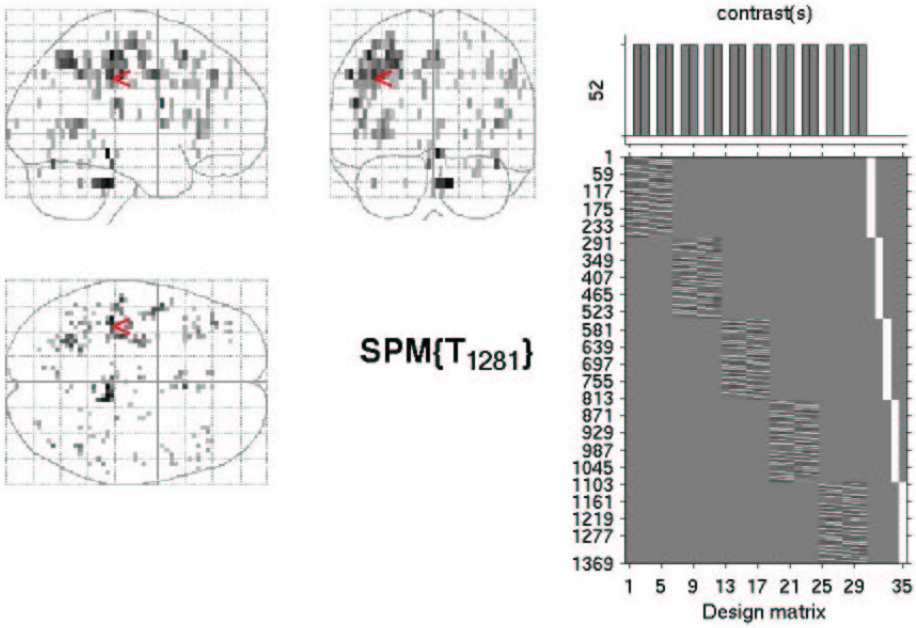

Figure 5.4 SPM_t map of the contrast function $+Ld + Lt + Hd + Ht - P$, exclusively masked by $+Ls - Ld + Lt + Hs - Hd + Ht$ (corrected. $p < 0.05$). Height threshold T = 5.12, extent threshold k=0. Time-slicing done with phase-shift method.

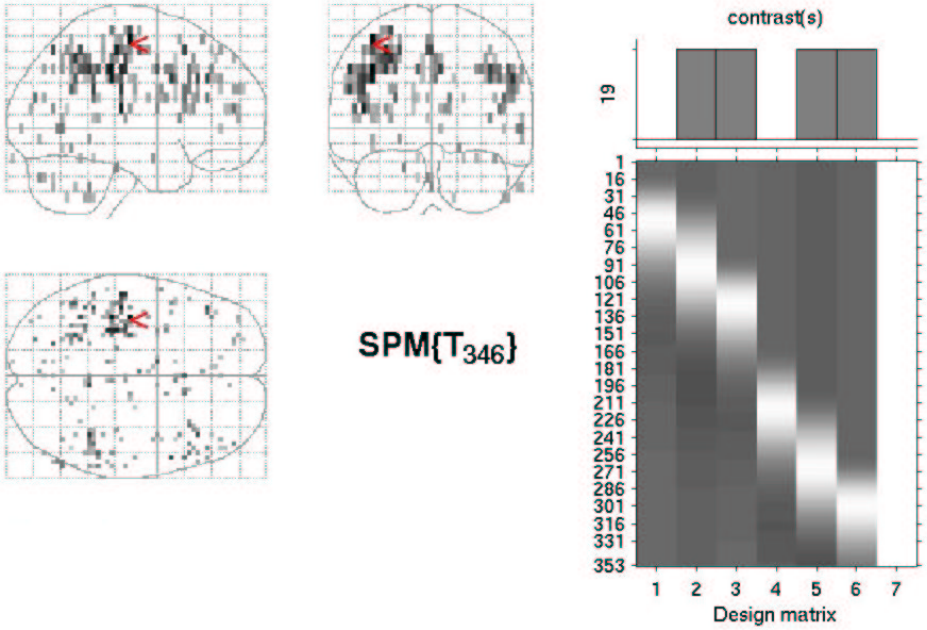

Figure 5.5 SPM_t map of the contrast function $+Ld + Lt + Hd + Ht - P$ exclusively masked by $+Ls - Ld + Lt + Hs - Hd + Ht$ (corrected, $p = 0.05$). Height threshold T=5.04, extent threshold k=0. DLS-re-sorted data.

5.5.4 Results of the Group Analysis

A group analysis can reveal effects similarly expressed in several group members, even if hidden by signal variability in individual data sets. The rationale of a group analysis is simply that group effects add up, while those signal components are averaged out that vary over the subjects.

Linear regression in the GLM was again used on the group data for cross-checking. We used the same combination of contrasts in the GLM as for the single subject analysis in section 5.5.3. Unlike in the single subject, where no functional activity could be detected, delay activation was found in the group analysis, see figure 5.6.

The cluster centers resulting from the TCA of the group data are displayed in figure 5.8. First we asked for spatial similarities between the high load clustering results and the SPM_t map of figure 5.6. The best and the second best matches to the SPM_t map were the clusters $H12$ and $H10$, reaching together a spatial similarity to the SPM_t map of $ss = 0.077$. Their spatial maps are displayed in figure 5.7.

Figures 5.6 and 5.7 reveal a qualitative agreement. Both spatial maps were dominantly located in the left superior parietal cortex (BA40), in regions at the midline, superior frontal gyrus (BA6) and in the left prefrontal cortex (BA9). Furthermore, the time courses of $H12$ and $H10$ were similiar to each other, and showed, in fact, delay activity; a pronounced peak in the second half of the delay period, see figure 5.8. Thus, the TCA found components with qualitative spatial

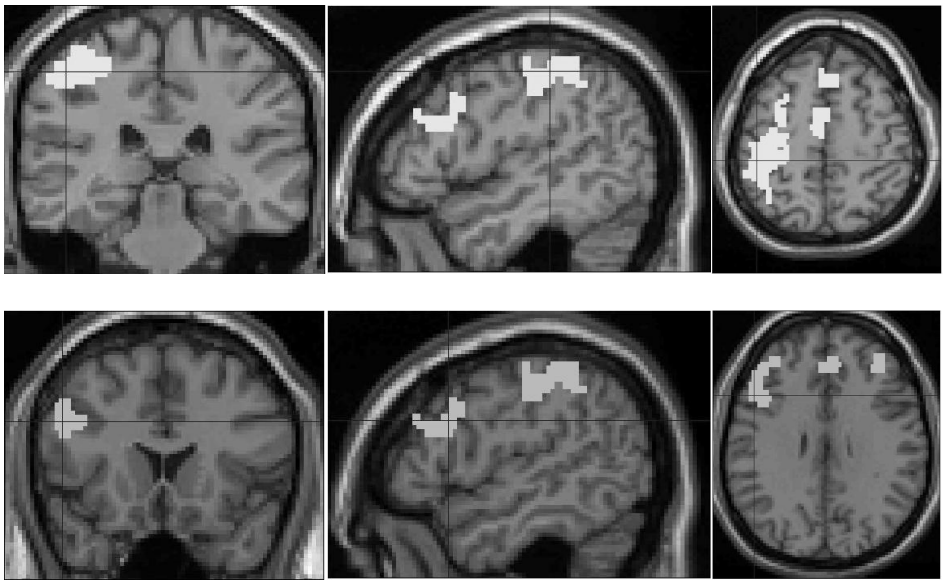

Figure 5.6 SPM_t map of the contrast $-Hs + Hd$, masked exclusively by $Hs - P$, and by $+Ld - Hd$ (corrected, $p = 0.05$). In the upper row the cursor position is in BA40, in the lower row in BA9. Phase-shift time-slicing used.

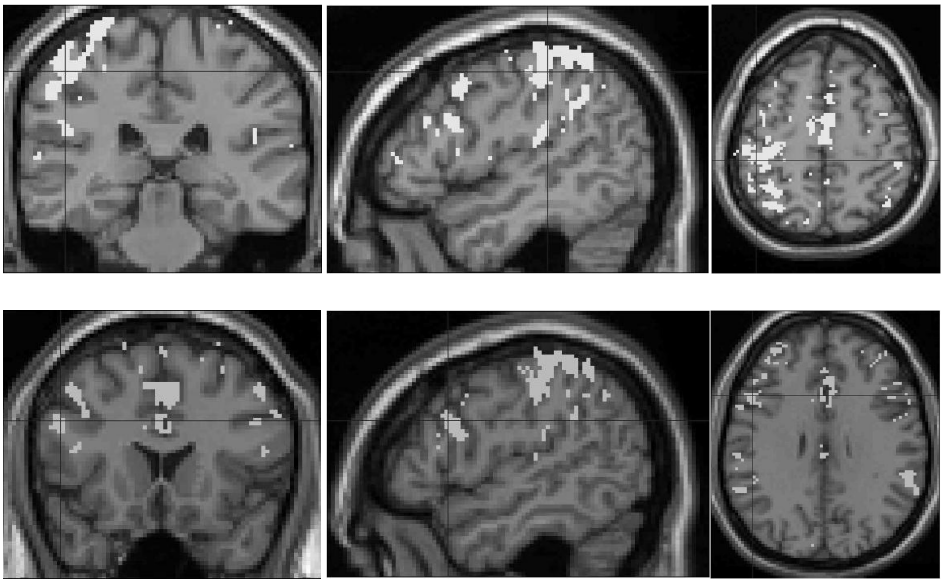

Figure 5.7 Spatial maps of $H10$ and $H12$, the clusters with highest spatial overlap with the SPM_t map of figure 5.6. Both cluster centers show a pronounced peak in the late delay period, see figure 5.8. In the upper row the cursor position is in BA40, in the lower row in BA9. DLS-re-sorting used for slice timing.

similarity to the SPM map. The detailed patterns of activity, however, deviated: the spatial similarity ss between the TCA clusters and the SPM_t stayed far below one, and at some regions they disagreed considerably. The spatial cluster located in right prefrontal cortex in the SPM map, for instance, had only some scattered voxels as counterparts in the TCA result. Differences must be caused by the different ways of data analysis and preprocessing as well. One should be aware, that there is no "gold standard" for analyzing these data. The mutual masking of contrasts used to generate the SPM_t map is just another way of exploratory data analysis.

The crucial question is now what the exploratory analysis technique based on cluster analysis can reveal about the expression of delay activity exceeding the scope of GLM-based data analysis. For the systematic assessment of the entire clustering results we proceeded as described in the sections 5.4.2.3 and 5.4.2.1. First, we selected clusters with high signal change homogeneity. The chosen selection threshold was $SCH \geq 2.6$, which was surpassed by 7 clusters for high, and 8 for low load condition. One low load cluster was excluded because of lacking temporal smoothness. The cluster centers of 11 of the selected clusters are displayed in figure 5.8. Among the selected high load clusters were the previously described "delay activity" clusters $H12$ and $H10$, but also $H15$, with quite similar activation time course, peaked in the late delay. There were more clusters displaying activation during the delay, however, with quite different time course: The signal courses of $H2$ and $H16$ show not only activation in the delay period but also in the phase of

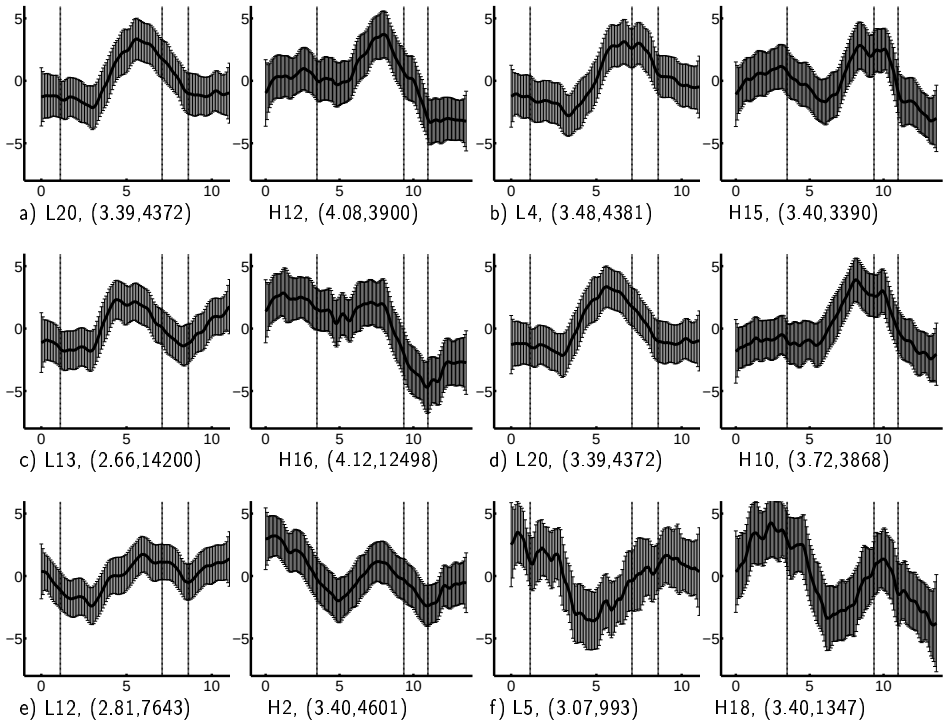

Figure 5.8 Cluster centers obtained by the analyses of high and low load trials. The displayed clusters satisfied our selection criteria based on the measures SCH and TCH (defined in section 5.4.2.3). High and low load clusters are paired with respect to high spatial similarity. Each pair a) to f) shows on the left the center for low load and on the right the center for high load. The horizontal axes display latency time with respect to stimulus onset (in seconds, $t = 0$ marks the canonical hemodynamic delay interval of 5s after stimulus onset). The curve onsets mark the begin of the phase s, the three bars indicate transitions between the phases s, d, t and P. The vertical axes display relative signal strength (in arbitrary units). Error bars represent the signal standard deviation within the cluster. Below each diagram one finds the name of the cluster, and in brackets, the SCH value and cluster size (in voxels). The pairs a) to f) are ordered with respect to decreasing spatial similarity (ranging from $ss = 0.156$ for a), to $ss = 0.127$ for f).

memory set presentation. The time course of $H2$ displayed an activity peak in the late delay period quite similar to the cluster centers of $H12$, $H10$ and $H15$, but there was a second activity peak in the preceeding period with visual stimulation. Of course, voxels with such temporal behavior remain undetected by the $d - s$ contrast used in the GLM-based data analysis. Figure 5.9 shows the spatial pattern of the cluster $H2$. The spatial pattern of cluster $H2$ was located in the upper left and right occipito-parietal cortex, (BA19, BA40).

Cluster $H16$ showed a signal time course that was quite unique among the clusters with increased activities in the delay. The signal was high during the visual stimulation and the activity persisted without interuption almost until to the end

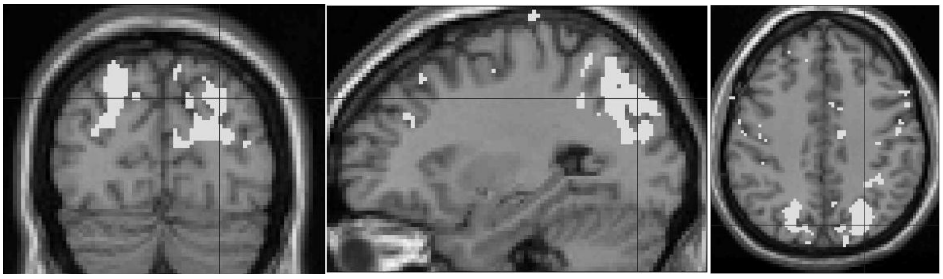

Figure 5.9 Map of cluster $H2$. It was activated in the stimulus and had a second peak in the delay. The cursor is set at the Talairach coordinates 27 -78.1 37.6 mm in BA19.

of the target period. The interpretation of this activation function is less clear since the prolonged activity could just be a confounding effect from the preceeding phase, but see discussion below.

So far, we have discussed the high load clusters showing pronounced effects in the delay period. To study load dependencies, we checked for spatial correspondences between high and low load clusters. We scored high/low load pairs with respect to spatial similarity. The spatial similarities ranged between $ss = 0.156$ and $ss = 0.0$. Interestingly, all 14 selected clusters belonged to the 10 high scored pairs, with spatial similarities higher than $ss = 0.098$. Eight of the 10 high scored pairs had a pairwise association, i.e., they were best-matching pairs, see definition in section 5.4.2.3. Figure 5.8 shows the six pairs with highest spatial similarity. With the exception of pair d), the clusters displayed in figure 5.8 were best-matching pairs. The pairs a) and d) associate the clusters $H12$ and $H10$ with the same low load cluster $L20$. Note that $H12$ and $H10$ were the both clusters with highest spatial similarity to the GLM map, see figure 5.7. The magnitudes of the spatial similarity within pairs already indicated a substantial overlap region[12] and a visually salient similarity.

Interestingly, in many cluster pairs, a), b), d), f), we found high similarity in signal shape and amplitude of the cluster centers. This indicated load-independent activation time courses in the overlap regions of these cluster pairs. The strongest load-dependency was observed in the overlap of pair c): While during low load the activity was peaked in the late delay ($L13$), the cluster $H16$, described above, showed persistent activity from stimulus to the end of the delay phase during high load. Since quite clearly $L13$ displayed delay-related activity, the region where $L13$ overlapped with $H16$ was likely to convey delay-related neuronal activity also during high load, even if this was unclear from the time course of $H16$ alone. The spatial pattern of the overlap region of cluster pair c) is shown in figure 5.10. It is spatially clustered in the precentral gyrus (BA6), bilateral near the midline (SMA), and left parietal cortex.

12. For instance, the overlap region of cluster pair c) is displayed in figure 5.10.

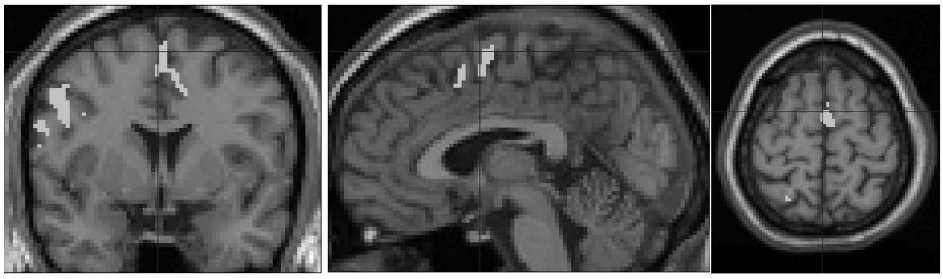

Figure 5.10 Voxels belonging to both clusters L13 and H16 of cluster pair c) showing the most extreme load-dependency in the activation. The cursor is set at the Talairach coordinates -2.2 1.4 61.0 mm in medial precentral gyrus (BA6).

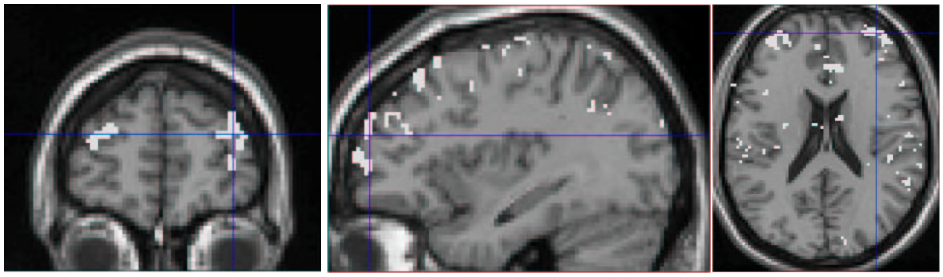

Figure 5.11 Load-dependent delay period specific effect. This map shows the voxels in the superset of high load clusters with delay peak (H10, H12, H15), but not in the superset of low load clusters with delay peak (L4, L20). The cursor is set at the Talairach coordinates 35.3 56.1 18.6 mm in the right BA10.

The spatial deviations within the cluster pairs cannot be interpreted directly, see section 5.4.2.1. For a rough estimation how the global region of exclusive delay activation changed with load we merged for each load all the clusters with the typical activity peak in the late delay/early target (the clusters in the pairs a, b, and d). The voxel ratio between high and low load was 1.27, indicating a slight load-dependent increase of the activated volume. We asked for the spatial distributions of load specific activation: The map of voxels with delay activation only in the high load, shown in figure 5.11, was clearly spatially clustered in prefrontal cortex and in gyrus cinguli anterior. The map of voxels with delay activation exclusively during the low load exhibited less pronounced spatial clusters located in premotor and posterior parietal regions (map not shown here).

5.6 Discussion

5.6.1 Relations to Other Exploratory Analysis Techniques for fMRI

A number of different exploratory analysis methods have been proposed for fMRI, e. g. cluster analysis, principal/independent component analysis, neural networks. These exploratory approaches have demonstrated that for block designs functional activity can be detected completely uninformed by the experimental paradigm, see references in section 5.4.2.

For event-related designs involving short events and different conditions, functional activation is unlikely to be found completely uninformed of the paradigm. Event-related effects are small compared to other signal influences and functional recruitment of different conditions might interfere with each other. Earlier studies applying explorative techniques on event-related experiments used previous knowledge about the task by introducing spatial constraints, i.e., restricting the analysis to regions of interests (Richter et al., 2000). The incentive of our technique is to explore the whole brain, by relying on temporal constraints dictated by experimental paradigm. In the case of the working memory study we applied TCA separately on data segments that corresponded to different load conditions.

Exploratory methods, though reducing raw data, still tend to produce data sets rich in structure (like the clusters obtained from temporal clustering as involved in our technique). Often, the a posteriori assessment of exploratory results is done more or less ad hoc and the selection of reported clusters does not rely on fair data-based criteria, but is biased by expectations about the results. We believe that a crucial component of exploratory data analysis is a systematic and fair a posteriori assessment of the reduced data sets. Therefore we introduced quantitative measures and similarity relations to select, evaluate and interprete the TCA clusters. We selected clusters with high signal change homogeneity SCH and high temporal smoothness TSM to account for functional activity[13]. However, once thresholds were fixed, all clusters were reported that fullfill the criterion.

The paradigm-informed application of TCA presented in this chapter actually increased the difficulty of a posteriori assessment. Instead of just one data partition we had to deal with different data partitions for each load condition. For a systematic assessment of load-dependent effects we scored the spatial similarity between cluster pairs. We found pairwise correspondences between most of the previously selected clusters. Thus, the assessment of load-dependencies mainly involved pairwise comparisons between clusters.

Various temporal clustering methods have turned out to perform well on fMRI data, see section 5.3. Biased by our previous experience, we chose a dynamical hard clustering algorithm (DCA) (Baune et al., 1999) and compared this approach with

13. In the displayed mean time courses we visualize by error bars the cluster homogeneity proposed earlier (Baumgartner et al., 1999).

faster clustering algorithms. Previously it had been shown that k-means cluster analysis with random initialization of the cluster seeds has lower robustness than DCA (Baune et al., 1999). We found that k-means clustering, if extended by an dynamical initialization phase (Waldemark, 1997), can achieve similar results and similar robustness as DCA. The dynamical initialization proved to be effective in preventing the gradient-descent to terminate in local minima.

Volume slice timing is an inevitable step of data preprocessing for exploratory data analysis based on temporal similarity. In common slice timing techniques (Aguirre et al., 1998) the signal interpolation is a potential source of signal distortion. Since the detection of functional activation during a working memory task with short delay is hard (low S/N), we wanted to eliminate as much as possible sources of noise in data preprocessing. We proposed dense latency sampling (DLS) that not only enhances time resolution by oversampling (Josephs et al., 1997; Miezin et al., 2000), but provided slice timing without introducing any signal interpolation errors. It should be noted that the re-sorting process of the DLS-technique destroys the auto-correlation structure of signal components that are unrelated to the events. However, this does not have a strong impact on the detection of event-related activity.

5.6.2 Probing Delay Related Activity: Methodological Issues

The slow HR characteristic is the limiting factor for the temporal resolution of regional cerebral blood-flow-based techniques including fMRI. A serious problem these techniques have with event-related data acquisition is to disentangle functional activity from different events following on each other in fast succession. In the case of event-related working memory studies, delay related activity might be confounded by the HR resulting from processes during the preceding presentation period. A way to exclude this confound is to prolong the delay period – e.g. to 12s – and to consider only delay activity occuring not earlier than 4-5s after the onset of the delay period, e.g. (Zarahn et al., 1997; Cohen et al., 1997; Postle et al., 1999; Rypma and D'Esposito, 1999; D'Esposito et al., 2000). However, this approach has major drawbacks, such as the qualitative changes of working memory with variation of the delay period, and the fact that experimental sessions become quite long.

In this study we examined a delayed response task with a delay period of 6s. The chosen delay length was still in the time domain of working memory most intensely studied by other experimental methods. Though the delay duration was on the short end of those examined by other neuroimaging studies, we were confident to detect delay-related activity for a number of reasons. Visual experiments had indicated almost linear summation for the hemodynamic responses of different events (Boynton et al., 1996; Buckner, 1998), and consecutive events have been successfully resolved, even if their time delay was only about $2-3$s (Kim et al., 1997). Burock et al. (1998) demonstrated that at fast stimulus presentation rates the hemodynamic responses could be estimated quite well. Moreover, confounding due to the HR is only a problem if successive events activate the same regions. Small

latencies (of the order of several hundreds of milliseconds) between different regions had been previously detected, for instance in regions involved in voluntary hand movement (Wildgruber et al., 1997; Baune et al., 1999). To provide the optimum power for detection of delay-specific activity, we tried to optimize experimental paradigm, design, and the exploratory technique: i) In order to restrict in both load conditions encoding processes to the period of memory set presentation, we adjusted the presentation time according to the number of items to be remembered, see section 5.5. ii) We eliminated possible distortions from signal interpolation by applying the DLS method. iii) In the GLM analysis we checked for delay activity against the activity level during stimulus presentation, and not against baseline. iv) The exploratory technique was unbiased by a priori hypotheses about the signal shape of functional activation. Such a bias reduces sensitivity in case of mismatch between hypothesis and actual activation.

5.6.3 Results on Working Memory

We examined a delayed response task with 6s delay duration and two different load conditions (1 versus 6 letters). In a single subject we found functional activation related to the phase including delay period and probe phase in parietal and prefrontal regions. However, none of the techniques found purely delay-related activation. The situation was different in the data averaged over 8 subjects. Here clear delay-specific activity was found, with the conventional slice timing and analysis technique (figure 5.6) and as well with the exploratory analysis technique (figure 5.7). Both analysis techniques located the delay activity accordingly in typical working memory regions, inferior parietal left, superior frontal left, superior medial (BA6) and bilateral prefrontal (BA9).

The exploratory technique yielded results going beyond those obtained by an inferential technique, mainly because the former can characterize functional activation unbiased by expected signal shapes (regressors) or locations (anatomically defined regions of interest[14]). Most delay-related activity found by the exploratory data analysis had a particular transient signal shape, a peak in the second half of the delay period (figure 5.8 a,b,d,L13). In some clusters the peak width was somewhat wider and involved some of the target period too (figure 5.8 b,H10). Since all these time courses involved no high activity in the preceeding visual stimulus period, confounding effects were no problem in indentifying these activity peaks as delay-related. In pre- and sensomotoric regions delay peaks were found during both load conditions (overlaps of the cluster pairs a, b and d in figure 5.8). In other regions delay peaks occurred load specifically: for high load in bilateral spatial clusters in PFC, and in anterior cingulate (figure 5.11). The latter regions seemed to be particularly involved in working memory related processes during the delay pe-

14. Jhi and McCarthy (2000) studied signal time courses during delayed tasks averaged over anatomically defined regions of interest.

riod. Since the activation occured in the later part of the delay period, they might participate in rehearsal as well as in preparation of the stored information to be used in desicion making. The left lateralization of delay-related activity (seen in Figs. 5.6 and 5.7) is in accordance to a number of studies on the processing of verbal material, see for instance (Awh et al., 1996; Gabrieli et al., 1998; Smith et al., 1997; Smith and Jonides, 1999).

Other clusters showed activity during the delay period as well, but the activation also included the preceeding period of memory set presentation (figure 5.8 $H2$,$H16$). The functional interpretation of these clusters relied on their detailed time courses or on spatial relationships between clusters of the different load conditions. One cluster center ($H2$) exhibited two peaks clearly separated in time, one during stimulus presentation and one during delay. This suggested that the delay activity is no confound from the preceeding phase, but a true delay-related component. The cluster was localized in bilateral superior parietal regions near midline. We conclude that superior parietal regions are not only involved in perception and encoding, but also in delay-locked processes of working memory, such as rehearsal. Another cluster ($H16$) allowed no functional assignment based on its signal shape, the activity was high during visual stimulation and persisted continously almost over the complete delay period. But for this cluster the best-matching cluster from the analysis of low load events ($L13$) showed peaked delay activity (figure 5.11 c). Thus, voxels in the overlap of $H16$ and $L13$ are likely to be involved in delay-related processes as well. These voxels were located in BA6, precentral and left lateral (figure 5.10). In BA6 the load dependency was largest during the period of visual stimulation. Thus, BA6 might participate in working memory maintainance, but its most important role is more likely to be in encoding.

In this paragraph we summarized results obtained with the explorative technique and how they can be interpreted in terms of process specific involvements of cortical regions. A more complete description and discussion of the results in the context of process specific theories of working memory (Baddeley, 1996), as well as the relation to other working memory studies, will be subject of a forthcoming paper.

5.6.4 Conclusions

We have described a technique of exploratory data analysis for ER fMRI experiments. The technique includes two components. The first component is a new oversampling and data sorting scheme (DLS: dense latency sampling. The second component is a paradigm-informed application of temporal cluster analysis to event-related data combined with a systematic evaluation of the clustering results. A dynamical variant of k-means analysis (K-MDI CA) permitted rapid and reproducible cluster analysis of the data.

The technique was used for a study of delayed response working memory. As a reference, we also used standard techniques to evaluate the same data set. At a macroscopic level, both methods gave a similar view of patterns of delay-related approaches gave similar results about. Thus important features of the results can

be extracted by methods that differ in the type of underlying assumptions—functional specialization versus functional integration. Furthermore, the exploratory technique yielded results that the standard technique could not provide. The exploratory technique was able to provide a global view of the spatio-temporal structure associated with each different type of event. Thus, it was possible to assess involvement of disparate regions in different process of working memory.

The time course of the delay-related activity that we found differed from that measured with single cell recordings. The delay-related activity we measured reached a peak over time while the firing rates of individual prefrontal cells is persistent, a pattern that is interpreted as memory maintainance. The difference between the results might come from the fact that fMRI signals reflect activity of functionally diverse populations of cells that are involved in several processes. Such processes could include rehearsal that sets in later in the delay and computations that prepare the decision process.

In additon, our results suggest that superior parietal visual areas might be not only involved in perception or encoding, but also in rehearsal or decision making. This finding is especially encouraging because the involvement of sensory areas in decision processes has recently been found in electrophysiological studies of working memory, see (Brody, 2002).

We hope to have been able to convince the reader that using exploratory analysis for event-related fMRI adds an interesting alternative to existing techniques. Further we advocated that paradigm-informed application of TCA and systematic assessment of clustering results allows exploratory data analysis without restriction to regions of interest as by Richter et al. (2000). Finally, we proposed a solution of the slice timing problem (a problem that must be solved before any type of exploratory data analyis can be done) that avoids artifacts introduced by the standard method.

We believe it is important to add a final remark about one caveat of multivariate analysis of fMRI at high temporal resolution. Current methods rely on the assumption that synchrony of the hemodynamic response in different voxels corresponds to synchrony of the underlying neuronal activity. This assumption becomes more and more questionable as temporal resolution is increased. Indeed, there is some evidence that the delay of the hemodynamic response can vary with location (Aguirre et al., 1998) and with type of stimulation (Friston et al., 1998). Thus, further advances in fMRI will depend on a better understanding of the relationship between the hemodynamic response and patterns of neural activity.

Acknowledgments

This work was supported by a Landesforschungsschwerpunktprogramm grant from the state of Baden-Württemberg and by Wilhelm-Schweizer-Zinnfiguren in Diessen.

References

G. K. Aguirre, E. Zarahn, and M. D'Esposito. The variability of human BOLD hemodynamic responses. *NeuroImage*, 8(4):360–369, 1998.

E. Awh, J. J. Jonides, E. E. Smith, E. H. Schumacher, R. A. Koeppe, and S. Katz. Dissociation of storage and rehearsal in verbal working memory: evidence from positron emmission tomography. *Psychological Sciences*, 7:25–31, 1996.

A. Baddeley. *Working Memory.* Oxford University Press, Oxford, England, 1986.

A. Baddeley. The fractionation of working memory. *Proceedings of the National Academy of Sciences USA*, 93:13468–13472, 1996.

P. A. Bandettini, A. Jesmanowicz, E. C. Wong, and J. S. Hyde. Processing strategies for time-course data sets in functional MRI of the human brain. *Magnetic Resonance in Medicine*, 30:161–173, 1993.

R. Baumgartner, L. Ryner, W. Richter, R. Summers, M. Jarmasz, and R. Somorjai. Comparison of two exploratory data analysis methods for fMRI: fuzzy clustering vs. principal component analysis. *Magnetic Resononance Imaging*, 18(1):89 – 94, 2000a.

R. Baumgartner, G. Scarth, C. Teichtmeister, R. Samorjai, and E. Moser. Fuzzy clustering of gradient-echo functional MRI in human visual cortex. part I: Reproducibility. *Journal of Magnetic Resonance Imaging*, 7:1094 – 1101, 1997.

R. Baumgartner, R. Somorjai, and W. Richter. Assessment of cluster homogeneity in fMRI data using Kendall's coefficient of concordance. *Journal of Magnetic Resononance Imaging*, 17(2):1525 – 1532, 1999.

R. Baumgartner, R. Somorjai, R. Summers, W. Richter, and L. Ryner. Correlator beware: Correlation has limited selectivity for fMRI data analysis. *NeuroImage*, 12(2):240–243, 2000b.

A. Baune, M. Erb, F. T. Sommer, D. Wildgruber, U. Klose, and W. Grodd. Evaluation of fast fMRI measurements in motorcortex: Comparing a new cluster analysis with z-mapping. *Exp. Brain Res.*, 117:50, 1997.

A. Baune, F. T. Sommer, M. Erb, D. Wildgruber, B. Kardatzky, and W. Grodd. Dynamical cluster analysis of cortical fMRI activation. *NeuroImage*, 6(5):477 – 489, 1999.

G. M. Boynton, S. A. Engel, G. H. Glover, and D. J. Heeger. Linear systems analysis of functional magnetic resonance imaging in human. *Journal of Neuroscience*, 16:4207 – 4221, 1996.

C. Brody. Dynamics of sensory area during sensory discrimination and decision task. Talk presented at *NICE 2002 workshop*, Les Houches, 2002.

R. L. Buckner. Event-related fmri and the hemodynamic response. *Human Brain Mapping*, 6(5-6):373–377, 1998.

M. A. Burock, R. L. Buckner, M. G. Wolfdorff, B. R. Rosen, and A. M. Dale. Randomized event-related experimental desighs allow for extremely rapid presentation rates using functional MRI. *Neuroreport*, 9:3735–3739, 1998.

M. A. Burock and A. M. Dale. Estimation and detection of event-related fmri signals with temporally correlated noise: A statistically efficient and unbiased approach. *Human Brain Mapping*, 11(4):249–260, 2000.

R. Cabeza and L. Nyberg. Imaging cognition II: an empirical overview of 275 PET and fMRI studies. *Journal of Cognitive Neuroscience*, 12(1):1–47, 2000.

J. D. Cohen, W. M. Perlstein, T. S. Braver, L. E. Nystroem, D. C. Noll, J. Jonides, and E. E. Smith. Temporal dynamics of brain activation during a working memory task. *Nature*, 386:604–608, 1997.

A. M. Dale. Optimal experimental design for event-related fMRI. *Human Brain Mapping*, 8(2-3):109–114, 1999.

A. M. Dale and R. L. Buckner. Selective averaging of rapidly presented individual trials using fMRI. *Human Brain Mapping*, 5(5):329–340, 1997.

M. D'Esposito, D. Ballard, E. Zarahn, and G. K. Aguirre. The role of prefrontal cortex in sensory memory and motor preparation: An event-related fMRI study. *NeuroImage*, 11(5):400–408, 2000.

M. D'Esposito, J. A. Detre, D. C. Alsop, R. K. Shin, S. Atlas, and M. Grossman. The neural basis of the central executice system of working memory. *Nature*, 378: 279–281, 1995.

M. D'Esposito, B. R. Postle, J. Jonides, and E. E. Smith. The neural substrate and temporal dynamics of interference effects in working memory as revealed by event-related functional MRI. *Proceedings of the National Academy of Sciences USA*, 96:7514–7519, 1999.

M.J. Fadili, S. Ruan amd D. Bloyet, and B. Mazoyer. A multistep unsupervised fuzzy clustering analysis of fmri time series. *Human Brain Mapping*, 10(4):160 – 178, 2000.

P. Filzmoser, R. Baumgartner, and E. Moser. A hierarchical clustering method for analyzing functional MR images. *Magnetic Resonance Imaging*, 17(6):817 – 826, 1999.

K. J. Friston, P. Fletcher, O. Josephs, A. P. Holmes, K. J. Worsley, M. D. Rugg, and R. Turner. Event-related fmri: characterizing differential responses. *Neuroimage*, 7(1):30–40, 1998.

John D. E. Gabrieli, Russell A. Poldrack, and John E. Desmond. The role of left prefrontal cortex in language and memory. *Proceedings of the National Academy of Sciences, U.S.A.*, 95:906–913, 1998.

X. Golay, S. Kollias, G. Stoll, D. Meier, A. Valavanis, and P. Boesiger. A new correlation-based fuzzy logic clustering algorithm for fmri. *Magn Reson Med*, 40: 249–260, 1998.

P. Goldman-Rakic. The prefrontal landscape: Implications of functional architecture for understanding of human mentation and the central executive. *Philosophical Transactions of the Royal Society B*, 351:1445–1453, 1996.

P. Goldman-Rakic. Localization of function all over again. *NeuroImage*, 11(5): 451–457, 2000.

C. Goutte, P. Toft, E. Rostrup, F. A. Nielsen, and L. K. Hansen. On clustering fMRI time series. *NeuroImage*, 9(3):298–310, 1999.

L. K. Hansen, J. Larsen, F. A. Nielsen, S. C. Strother, E. Rostrup, R. Savoy, N. Lange, J. Sidtis, C. Svarer, and O. B. Paulson. Generalizable patterns in neuroimaging: how many principal components? *NeuroImage*, 9(5):534–544, 1999.

R. N. A. Henson, C. Büchel, O. Josephs, and K. Friston. The slice-timing problem in event-related fMRI. *NeuroImage*, 9:125, 1999.

P. Jezzard and S. Clare. Sources of distortion in functional MRI data. *Human Brain Mapping*, 8(2-3):80–85, 1999.

A. P. Jhi and G. McCarthy. The influence of memory load upon delay-interval activity in a working-memory tast: an event related functional MRI study. *Journal of Neuroscience*, 12(Supplement 2):90–105, 2000.

J. Jonides, E. E. Smith, R. A. Koeppe, E. Awh, S. Minoshima, and M. A. Mintun. Spatial working memory in humans as revealed by PET. *Nature*, 363:623–625, 1993.

O. Josephs and N. A. Henson. Event-related funcitonal magnetic resonance imaging: modelling, inference and optimization. *Philosophical Transactions of the Royal Society of London B Biological Sciences*, 354:1215–1228, 1999.

O. Josephs, R. Turner, and K. Friston. Event-related fMRI. *Human Brain Mapping*, 5:243–248, 1997.

S.-G. Kim, W. Richter, and K. Ugurbil. Limitations of temporal resolution in functional MRI. *Magnetic Resonance in Medicine*, 37(4):631–636, 1997.

S. H. Lai and M. Fang. A novel local pca-based method for detecting activation signals in fmri. *Magnetic Resonance Imaging*, 17(6):827–836, 1999.

N. Lange. Statistical approaches to human brain mapping by functional magnetic resonance imaging. *Statistics in Medicine*, 15(4):389–428, 1996.

N. Lange. Empirical and substantive models, the Bayesian paradigm, and meta-analysis in functional brain imaging. *Human Brain Mapping*, 5(4):259–263, 1997.

N. Lange, S. C. Strother, J. R. Anderson, F. A. Nielsen, A. P. Holmes, T. Kolenda, R. Savoy, and L. K. Hansen. Plurality and resemblance in fMRI data analysis. *NeuroImage*, 10(3):282–303, 1999.

G. MCarthy, M. Luby, J. Gore, and P. Goldman-Rakic. Infrequent events transiently activate human prefrontal and parietal cortex as measured by functional MRI. *Journal of Neurophysiology*, 77:1630–1634, 1997.

M. J. McKeown, S. Makeig, G. G. Brown, T.-P. Jung, S. Kindermann, A. J. Bell, and T. J. Sejnowski. Analysis of fMRI by blind separation into independent spatial components. *Human Brain Mapping*, 6:160–188, 1998.

M. J. McKeown, S. Makeig, G. G. Brown, T.-P. Jung, S. S. Kindermann, A. J. Bell, and T. J. Sejnowski. Functionally independent components of early event-related potentials in a visual spacial attention task. *Philosophical Transactions of the Royal Society of London B Biological Sciences*, 354:1135–1144, 1999.

M. J. McKeown and T. J. Sejnowski. Independent component analysis of fMRI data: Examining the assumptions. *Human Brain Mapping*, 6:368–372, 1998.

F. M. Miezin, L. Maccotta, J. M. Ollinger, S. E. Petersen, and R. L. Buckner. Characterizing the hemodynamic response: Effects of presentation rate, sampling procedure, and the possibility of ordering brain activity based on relative timing. *NeuroImage*, 11(6):735–759, 2000.

P. P. Mitra, S. Ogawa, X. Hu, and K. Ugurbil. The nature of spatiotemporal changes in cerebral hemodynamics as manifested in functional magnetic resonance imaging. *Magn Reson Med*, 37:511–518, 1997.

E. Moser, M. Diemling, and R. Baumgartner. Fuzzy clustering of gradient-echo functional MRI in human visual cortex. part ii: Quantification. *Journal of Magnetic Resonance Imaging*, 7:1102–1108, 1997.

I Neath, G. D.A. Brown, M. Poirier, and C. Fortin. Short-term/working memory: An overview. *International Journal of Psychology*, 34(5/6):273 – 275, 1999.

A. M. Owen, A. C. Evans, and M. Petrides. Evidence for a two-pstage model of spatial working memory within the lateral frontal cortex: a positron emission tomography study. *Cerebral Cortex*, 6:31–38, 1996.

K. M. Petersson, T. E. Nichols, J. B. Poline, and A. P. Holmes. Statistical limitations in functional neuroimaging. i. non-inferential methods and statistical models. *Philosophical Transactions of the Royal Society of London B Biological Sciences*, 354:1239–1260, 1999a.

K. M. Petersson, T. E. Nichols, J. B. Poline, and A. P. Holmes. Statistical limitations in functional neuroimaging. ii. signal detection and statistical inference. *Philosophical Transactions of the Royal Society of London B Biological Sciences*, 354:1261–1281, 1999b.

B. R. Postle, , and M. D'Esposito. Evaluating models of the topographical organization of working memory function in frontal cortex with event-related fMRI. *Psychobiology*, 28:132–145, 2000a.

B. R. Postle, J. S. Berger, and M. D'Esposito. Functional neuroanatomical double dissociation of mnemonic and executive control processes contributing to working memory performance. *Proceedings of the National Academy of Sciences, U.S.A.*, 96:12959–12964, 1999.

B. R. Postle, E. Zarahn, and M. D'Esposito. Using event-related fmri to asses delay-period activity during performance of spatial and nonspatial working memory tasks. *Brain Research Protocolls*, 1:57–66, 2000b.

G. Rainer, W. F. Asaad, and E. K. Miller. Memory fields of neurons in the primate prefrontal cortex. *Proceedings of the National Academy of Sciences USA*, 95: 15008–15013, 1998.

J. T. E. Richardson, R. W. Engle, L. Hasher, R. H. Logie, E. R. Stoltzfus, and T. Zacks. *Working Memory and Human Cognition.* Oxford University Press, Oxford, England, 1996.

W. Richter, R. Somorjai, R. Summers, M. Jarmasz, R. S. Menon, J. S. Gati, A. P. Georgopoulos, C. Tegeler, K. Ugurbil, and S.-G. Kim. Motor area activity during mental rotation studied by time-resolved single-trial fMRI. *Journal of Cognitive Neuroscience*, 12(2):310–320, 2000.

B. R. Rosen, Randy L. Buckner, and Anders M. Dale. Behind the scenes of functional brain imaging: A historical and physiological perspective. *Proceedings of the National Academy of Sciences, U.S.A.*, 95:773–780, 1998.

J. B. Rowe, I. Toni, O. Josephs, R. S. J. Frackowiak, and R. E. Passingham. The prefronatal cortex: response selecthion or maintainance. *Science*, 288:1656–1660, 2000.

B. Rypma and M. D'Esposito. The roles of prefrontal brain regions in components of working memory: effects of memory load and individual differences. *Proceedings of the National Academy of Sciences, U.S.A.*, 96(11):6558–6563, 1999.

G. Scarth, M. McIntire, B. Wouk, and R. L Samorjai. Detecxtion of novelty in functional images using fuzzy clustering. *Proceedings of the Society of Magnetic Resonance*, 3rd Sci. Meeting:238, 1995.

T. Schanze. Sinc interpolation of discrete periodic signals. *IEEE Transactions on Signal Processing*, 43(6):1502–1503, 1995.

E. E. Smith and J. J. Jonides. Storage and execution in the frontal lobes. *Science*, 283:1657–1661, 1999.

E. E. Smith, J. J. Jonides, C. Marshuetz, and R. A. Koeppe. Components of verbal working memory: evidence from neuroimaging. *Proceedings of the National Academy of Sciences USA*, 95:875–882, 1997.

J. Waldemark. An automated procedure for cluster analysis of multivariate satellite data. *International Journal of Neural Systems*, 8(1):3–15, 1997.

A. Wichert, A. Baune, G. Grön, H. Walter, and F. T. Sommer. Interpretation of event-related fMRI using cluster analysis. In V. Kurkova, N. C. Steele, R. Neruda, and M. Karny, editors, *Artificial Neural Nets and Genetic Algorithms*, 446–448. Springer, Wien, 2001a.

A. Wichert, H. A. Kestler, H. Walter, G. Grön, A. Baune, J. Grothe, A. Wunderlich, and F. T. Sommer. Explorative detection of delay activity during a working memory task. In G. M. Papadourakis, editor, *Proc. 4th Int. Conference on Neural Networks and Expert Systems in Medizine and Healthcare*, 266–271. Technological Educational Institute of Crete, Heraklion, 2001b.

D. Wildgruber, M. Erb, U. Klose, and W. Grodd. Sequential activation of suplementary motor area and primary motor cortex during self-paced finger movement in human evaluated by functional neural MRI. *Neuroscience Letters*, 227:1–4, 1997.

J. Xiong, J.-H. Gao, J.L. Lancaster, and P. T. Fox. Clustered pixel analysis for functional MRI activation studies of the human brain. *Human Brain Mapping*, 3:287–301, 1995.

E. Zarahn, G. K. Aguirre, and M. D'Esposito. Empirical analyses of BOLD fMRI statistics. I. Spatially unsmoothed data collected under null-hypothesis conditions. *NeuroImage*, 5(2):179–197, 1997.